ELSEVIER

Experimental Thermal and Fluid Science 20 (1999) 45–54

Experimental Thermal and Fluid Science

www.elsevier.nl/locate/etfs

Experimental research of fluid flow and convection heat transfer in plate channels filled with glass or metallic particles

Pei-Xue Jiang *, Zhan Wang, Ze-Pei Ren, Bu-Xuan Wang

Department of Thermal Engineering, Tsinghua University, Beijing 100084, People's Republic of China

Received 1 April 1998; received in revised form 1 June 1999; accepted 8 June 1999

Abstract

Fluid flow and forced convection heat transfer was investigated experimentally in a plate channel filled with glass, stainless steel or bronze spherical particles. The test section was 58 mm × 80 mm × 5 mm with water as the working fluid. The local wall temperature distribution was measured along with the inlet and outlet fluid temperature and pressures. The porous media greatly increased the heat transfer coefficient although the hydraulic resistance was increased even more. The effects of particle diameter, particle thermal conductivity and fluid velocity were examined for a wide range of thermal conductivities (from 75.3 W/(mK) for bronze to 0.744 W/(mK) for glass) and for three nominal particle sizes (0.278, 0.428 and 0.7 mm). The coolant water flow rate in the porous plate channel ranged from 0.01568 to 0.1992 kg/s. The Nusselt number and the heat transfer coefficient increased with decreasing bronze particle diameter, but decreased with decreasing glass particle diameter. A modified criterion was developed to judge the effect of d_p on the heat transfer coefficient. The Nusselt number and the heat transfer coefficient increased with increasing thermal conductivity of the packing material.

Keywords: Convection heat transfer; Porous plate channel; Heat transfer enchantment; Friction factor; Glass particles; Metallic particles

1. Introduction

Heat transfer enhancement techniques play a very important role in thermal control technologies used in microelectronic chips, powerful laser mirrors, aerospace craft, thermal nuclear fusion, etc. It is widely recognized that heat transfer can be intensified by increasing the surface area in contact with the coolant. Tuckerman and Pease [1,2] pointed out that for laminar flow in confined channels, the heat transfer coefficient is inversely proportional to the width of the channel since the limiting Nusselt number is constant. They built a water-cooled integral heat sink with microscopic flow channels, typically 50 μm wide and 300 μm deep, and demonstrated that extremely high power density circuits could be cooled with a surface flux of 790 W/cm^2 or more. Mahalingam [3] confirmed the superiority of microchannel cooling on a silicon substrate with a surface area of 5 cm×5 cm using water and air as coolants. In recent years many researchers have studied the heat transfer augmentation produced by microchannels.

Porous structures are another effective heat transfer augmentation technique. Porous structures intensify the mixing of the flowing fluid and enhance the convection heat transfer. Several cooling systems using porous structures have been applied to cooling mirrors in powerful lasers [4,5] and cooling phased-array radar systems [6]. Very high heat fluxes (4×10^7 W/m^2)can be obtained using single-phase water flow [5]. Chrysler and Simons [7] suggested the use of packed beds of spherical particles to enhance convective heat transfer from microelectronic chips while Kuo and Tien [8] suggested the use of foam metal for the same application. Jeigarnik et al. [9] and Haritonov et al. [4] theoretically and experimentally investigated convection heat transfer on flat plates and in channels filled with porous material such as sintered spherical particles, nets, porous metal, and felts. The working fluid entered or left the test section through several channels which were perpendicular to the test section. Most of their experimental data was for convection heat transfer in sintered bronze porous layers with different thickness (0.86–3.9 mm) and particle

* Corresponding author. Tel.: +86-10-62784530; fax: +86-10-62770209.

E-mail address: jiangpx@tsinghua.edu.cn (P-X. Jiang)

0894-1777/99/$ - see front matter
PII: S0894-1777(99)00030-8

diameters (0.1–0.6 mm). They found that the porous media increased the heat transfer coefficient 5–10 times although the hydraulic resistance was increased even more [9]. Lage et al. [6] studied a low permeability microprobe heat sink for cooling phased-array radar systems. Their results suggest an increased overall heat transfer coefficient could be obtained that would reduce the operational temperature of the electronics for the same waste heat generation rate. Hwang and Chao [10] experimentally and numerically studied convection heat transfer in sintered porous channels. Nasr et al. [11] experimentally studied forced convection heat transfer from a circular cylinder embedded in a packed bed of spherical particles showing that the packed bed greatly increased the Nusselt number (up to seven times for aluminum spheres).

Fluid flow and convection heat transfer in porous media have received much attention in the past five decades. The influences of such effects as non-Darcian effects, variable porosity, variable thermal physical properties, and thermal dispersion in the porous medium on the fluid flow and heat transfer have been widely studied [12–20]. There are yet some problems that still need to be investigated further. For example, according to Refs. [13–15,18] the heat transfer increases as the particle diameter increases, but Jeigarnik et al. [9], Hwang and Chaos [10] and Nasr et al. [11] found the opposite result. The possible non-monotonic variation of the convection heat transfer coefficient as the particle diameter, d_p, increases was analyzed theoretically by Jiang et al. [19], however, the variation needs to be verified experimentally. Moreover, the effects of thermal conductivity, particle diameter and fluid velocity on the convection heat transfer need to be studied further to optimize heat transfer augmentation technology using porous media.

The present paper reports the results of an experimental study of fluid flow and forced convection heat transfer in a plate channel filled with metallic or non-metallic spherical particles. The effects of particle diameter, particle thermal conductivity and flow velocity on the convection heat transfer were examined.

2. Experimental apparatus and data reduction

The geometry of the test section is depicted schematically in Fig. 1. The size of the heated test section was 58 mm × 80 mm × 5 mm. The upper plate of the channel received a constant heat flux, q_w, while the bottom and side plates were adiabatic. The flow entered the channel with an average velocity, u_o, and constant temperature, T_{of}. Adiabatic sections in the porous plate channel (1 mm long) were placed before and after the heated section. The coolant water flow rate in the porous channel ranged from 0.01568 to 0.1992 kg/s.

The experimental apparatus, shown schematically in Fig. 2, consisted of a water tank, a pump, a high level water tank, a test section, a heat exchanger, and

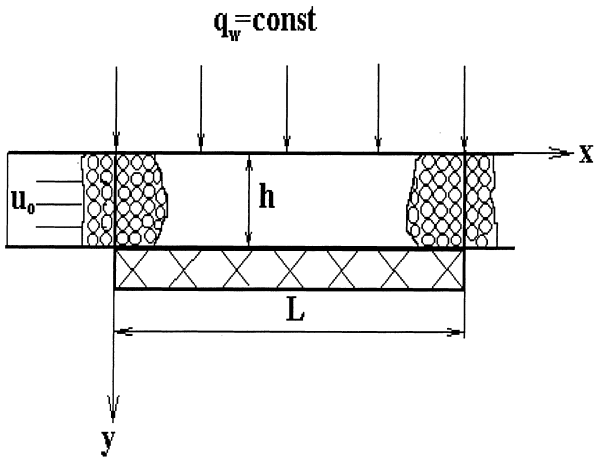

Fig. 1. Schematic diagram of the physical system.

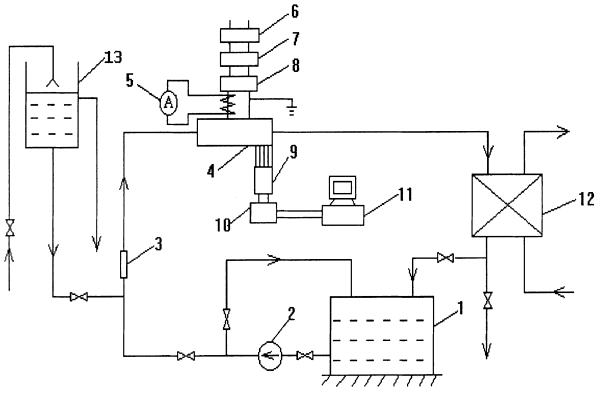

Fig. 2. Experimental apparatus: 1 – water tank; 2 – pump; 3 – filter; 4 – test section; 5 – current meter; 6 – voltage stabilizer; 7 – voltage regulator; 8 – transformer; 9 – multiplexer; 10 – digital multimeter; 11 – personal computer; 12 – plate heat exchanger; 13 – high level water tank.

instrumentation to measure temperatures, pressures and electrical power inputs. The high level water tank was used to verify the accuracy of the experimental system for an empty plate channel with small mass flow rates. The test section was made from a pure copper plate by wire machining and was thermally insulated from the outside environment. The upper plate of the test section was 2.5 mm thick. The plate channel was filled with packed metallic (stainless steel or bronze) or non-metallic (glass) particles. Three nominal bead diameters, 0.278, 0.428, or 0.7 mm were used in the experiments. Special care was taken in packing the beads to ensure uniformity in the structure of the porous medium. The spheres were poured randomly into the channel, leveled and then shaken. This procedure was repeated until no more beads could be placed into the channel. The spheres were supported by two perforated plates and fine mesh stainless steel screens at the inlet and outlet of the test section.

The upper plate was heated by a 0.4 mm thick plate heater using low-voltage alternating current to simulate a heat sink with constant heat flux. A mica sheet was placed between the heater and the plate channel surface. The small air gap between the mica sheet and the plate channel surface was filled with a high thermal conductivity paste to minimize the contact resistance. The heater voltage and current were measured by digital multimeters. The electric power input to the heater was calculated from the measured current and voltage readings.

The local temperature of the plate channel was measured with 18 copper–constantan thermocouples. Thirteen thermocouples were inserted into the upper plate of the test section (2 mm deep) along the centerline. Five more thermocouples were inserted into the upper plate of the test section (2 mm deep) along a line 2.0 cm away from the centerline to monitor the temperature variations across the test section. The inlet water temperature was measured by a thermocouple located at the inlet, approximately 4.5 cm upstream from the heated section. Three thermocouples were located at the outlet of the plate channel, approximately 4.5 cm downstream from the heated section and one thermocouple was located in the tube 17.5 cm downstream from the heated section to measure the bulk temperature at the exit. Prior to installation, the thermocouples were calibrated using a constant-temperature oil bath. The overall accuracy was well within ±0.2°C. The pressures at the inlet and outlet measured using accurate manometers with an accuracy of 0.25% of the full scale range of 1.6 MPa. The mass flow rate was measured by weighing the fluid flowing from the channel for a given time period.

Water was used as the working fluid. For each test, the flow rate, input power and inlet fluid temperature were fixed. The temperatures were measured with 23 thermocouples connected through a multiplexer to a digital multimeter (HP34401A) and a personal computer. The temperatures were monitored and recorded after steady-state conditions were reached. The flow rate, inlet and outlet fluid bulk temperatures, and electric current and voltage across the heater were also recorded. The local bulk mean temperature of the fluid at the measuring section was calculated from the inlet temperature, flow rate and power input, or from the inlet and outlet temperatures using linear interpolation. The fluid enthalpy rise was checked against the electric power input. The experimental uncertainty in the heat balance were ±7%.

The bulk porosity of the porous medium (packed bed) was computed for each run according to the following definition:

$$\varepsilon_{\mathrm{m}} = \frac{V_{\mathrm{t}} - V_{\mathrm{p}}}{V_{\mathrm{t}}}. \tag{1}$$

The local heat transfer coefficient, h_x, and Nusselt number, Nu_x, at each axial location were calculated as

$$\begin{aligned} h_x &= q_{\mathrm{w}}/(T_{\mathrm{wx}} - T_{\mathrm{fb}}), \\ Nu_x &= h_x D_{\mathrm{e}}/k_{\mathrm{f}}. \end{aligned} \tag{2}$$

The mean heat transfer coefficient, h_{m}, and mean Nusselt number, Nu_{m}, in the plate channel were calculated as

$$\begin{aligned} h_{\mathrm{m}} &= q_{\mathrm{w}}/(T_{\mathrm{wm}} - T_{\mathrm{fm}}), \\ Nu_{\mathrm{m}} &= h_{\mathrm{m}} D_{\mathrm{e}}/k_{\mathrm{m}}, \\ D_{\mathrm{e}} &= 2hW/(h + W). \end{aligned} \tag{3}$$

The local temperature of the heat transfer surface was calculated using the measured temperatures of the wall

$$T_{\mathrm{wx}} = T_x - \frac{q_{\mathrm{w}}\delta}{k}. \tag{4}$$

The mean temperature of the heat transfer surface was calculated as the average of all the centerline temperatures

$$T_{\mathrm{wm}} = \frac{\sum_{i=1}^{13}(T_{\mathrm{wx}}\Delta x)_i}{L}. \tag{5}$$

The mean fluid temperature, T_{fm}, was defined as the average value of the inlet and outlet fluid temperatures. The local bulk fluid temperature, T_{fb}, was calculated using

$$T_{\mathrm{fb}} = T_{f0} + \frac{q_{\mathrm{w}}}{Gc_{\mathrm{p}}} Wx \tag{6}$$

The pressure drop was calculated as

$$\Delta P = P_{\mathrm{in}} - P_{\mathrm{out}}. \tag{7}$$

The Reynolds number was defined as

$$Re_D = uD_{\mathrm{e}}/v_{\mathrm{m}}. \tag{8}$$

Preliminary tests were performed for data calibration and error estimate. The errors in the temperature measurements were due to inaccuracies in the initial calibration of the thermocouples and the recorder readings. The root mean square method was used to propagate errors for calculated quantities. The maximum uncertainty for the temperature measurement was within ±0.2°C. The uncertainty of the local temperature of the heat transfer surface, T_{wx}, was estimated to be ±0.207°C from Eq. (4) and the uncertainty of the local bulk fluid temperature, T_{fb}, was ±0.245°C from Eq. (6). The experimental uncertainty in the flow rate was ±1.5%. The experimental uncertainty in the pressure drop across the test section was ±6.5%. The experimental data collection procedure was carefully repeated for each test run. Steady-state was defined as the time when the deviations of the wall temperatures and the inlet and outlet temperatures were all within ±0.5°C for 20 min. The experimental uncertainty in the convection heat transfer coefficient, mainly due to experimental errors in the heat balance, the contact resistance between the plate heater and the test section plate surface, axial thermal conduction in the copper plate test section, the temperature measurements and the calculation of the heat transfer surface temperature, was estimated to be ±12.3%.

3. Results and discussion

The experimental investigation used three different particle materials, glass, stainless steel and bronze, and three nominal particle sizes (0.278, 0.428 and 0.7 mm). The thermal conductivities of these materials are 0.744, 16.4 and 75.35 W/(mK). The mean porosities for the different cases are listed in Table 1.

3.1. Test setup evaluation

The experimental setup was evaluated by comparing the results obtained for convection heat transfer in a empty plate channel with established correlations and numerical simulations. The range of the mass flow rates in the experiments in the empty plate channel was $0.0132 \sim 0.576$ kg/s, the corresponding Reynolds numbers were $369 \sim 12057$. Therefore, data was obtained for laminar, turbulent and transition flow. For laminar flow ($Re_D < 2300$) the convection heat transfer in an empty plate channel was calculated numerically. The local Nusselt numbers for turbulent and transition convection heat transfer in an empty plate channel were calculated using the formulas proposed by Petukhov et al. [21,22] and Gnielinski [21]

$$\frac{Nu_x}{Nu_\infty} = 1 + 0.416\ Pr^{-0.4}\left(\frac{x}{d}\right)^{-1/4}\left(1 + \frac{3600}{Re_D\sqrt{x/d}}\right) \times \exp\left(-0.17\frac{x}{d}\right) \left(\text{for } 4000 \leqslant Re_D \leqslant 10^6, 0.7. \leqslant Pr \leqslant 100, \frac{x}{d} > 0.5\right), \tag{9}$$

where,

$$Nu_\infty = \frac{(\zeta/8)Re_D Pr}{1 + 900/Re_D + 12.7\sqrt{\zeta/8}(Pr^{2/3} - 1)} \tag{10}$$

$$(\text{for } 10^4 \leqslant Re_D \leqslant 5 \times 10^6;\ 0.5 \leqslant Pr \leqslant 5 \times 10^5),$$

$$Nu_\infty = \frac{(\zeta/8)(Re_D - 1000)Pr}{1 + 12.7\sqrt{\zeta/8}(Pr^{2/3} - 1)} \tag{11}$$

$$(\text{for } 2300 \leqslant Re_D \leqslant 10^4;\ 0.5 \leqslant Pr \leqslant 200),$$

$$\zeta = (1.82\ \log Re_D - 1.64)^{-2}.$$

Fig. 3 shows the experimental results compared with the calculated results using Eqs. (9)–(11) and numerical simulations for various Reynolds numbers. The standard deviation between the experimental results and the predictions of Eqs. (9)–(11) and the numerical simulation was ±16.7%. The experimental uncertainty near the inlet and outlet is relatively large due to longitudinal thermal conduction along the test section which makes the experimentally determined heat transfer coefficients near the inlet less than the analytical values, and the experimental heat transfer coefficients near the outlet larger than the analytical values. In addition, Eqs. (9)–(11) are not very accurate near the inlet. In general, the accuracy of the experimental system is acceptable.

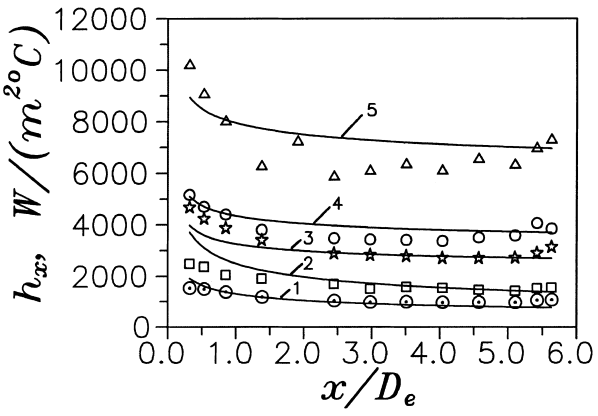

Fig. 3. Comparison of measurements with predictions for the empty plate channel ⊙, □, ☆, ◯, ◁ – – experimental data; ––– predicted values G[kg/s], Re_D: 1(⊙) – 0.0132, 369; 2(□) – 0.0830, 2215; 3(☆) – 0.2056, 4534; 4(◯) – 0.3086, 6456; 5(◁) – 0.5764, 12057.

3.2. Pressure drop and friction factor

Since the small spheres were supported by two perforated plates and fine mesh stainless steel screens at the inlet and outlet of the test section, the experimentally measured pressure drop between the inlet and outlet included the additional pressure loss resulting from the perforated plates and the fine mesh stainless steel screens. This component of the pressure drop was obtained experimentally using the empty plate channel with the perforated plates and the screens, Fig. 4. The data can be correlated using a least squares analysis as

$$\Delta P = 0.00634\ \mathrm{e}^{12.09G} \quad [\text{MPa}]. \tag{12}$$

Table 1
Experimental parameters

Particle material	Mean diameter d_p(mm)	Porosity ε_m (%)	Groups of experiment
Empty channel		100	30
Bronze	0.428	36.49	9
Bronze	0.278	34.10	5
Stainless steel	0.428	36.45	7
Stainless steel	0.7	37.90	5
Glass	0.428	36.61	5
Glass	0.7	37.81	5

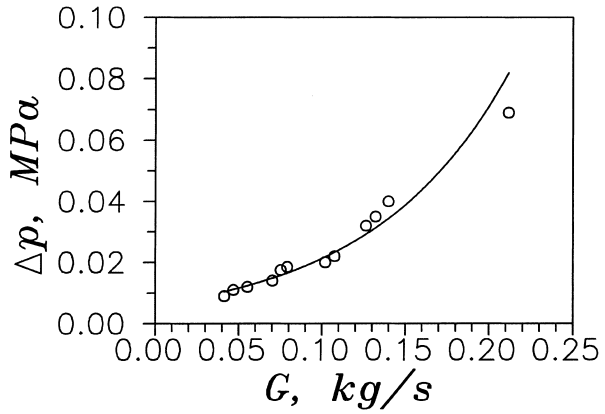

Fig. 4. Pressure drop with the perforated plates and screens.

The pressure drop for the porous media is the measured pressure drop minus the additional pressure loss. Fig. 5 shows the pressure drop in the porous plate channel as a function of mass flow rate. The pressure drop was greatly increased by the packed bed and increases as the particle diameter decreases. As shown in Table 1, the porosities for a given particle diameter and different materials were nearly the same in the present work. Therefore, the effect of porosity on pressure drop could not be verified with the present data. Jeigarnik et al. [9] found that the pressure drop greatly increased with decreasing particle diameter and porosity, but the influence of channel height on the pressure drop was not observed.

Fig. 6 compares the friction factor, f_e, calculated from the experimental data with the friction factor predicted using the equation given by Aerov and Tojec [23]

$$f_e = \frac{\varepsilon_m^3}{1-\varepsilon_m}\frac{\rho_f d_p}{3M^2}\frac{\Delta p}{L} = \frac{36.4}{Re_e} + 0.45 \quad (\text{for } Re_e < 2000). \tag{13}$$

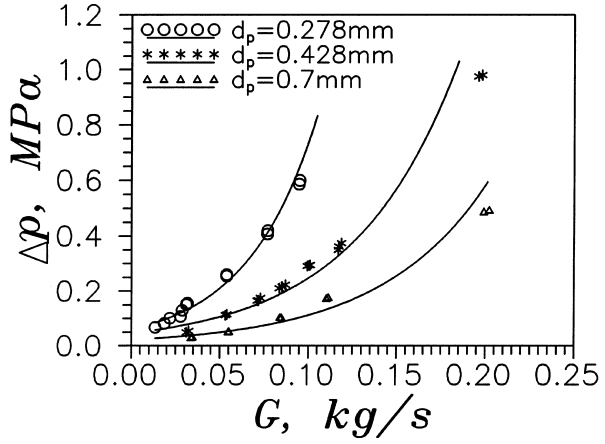

Fig. 5. Pressure drop along the porous plate channel.

The experimental values of f_e agree well with the values predicted using Eq. (13).

3.3. Local heat transfer coefficients and heat transfer enhancement due to the particles

Figs. 7–9 show the distribution of the local heat transfer coefficients for glass, stainless steel and bronze packed beds. The local heat transfer coefficients decrease along the axial direction and increase as the Reynolds number increases. The porous media greatly increased the heat transfer coefficient compared to the empty channel. For the glass packed bed, the heat transfer coefficient was enhanced 5–7 times; for stainless steel, 6–8 times and for bronze, 7–12 (compared to 8–10 times as found by Jeigarnik et al. [9] for sintered porous channels). The following analysis explains why the smaller bronze particles give higher heat transfer coefficients,

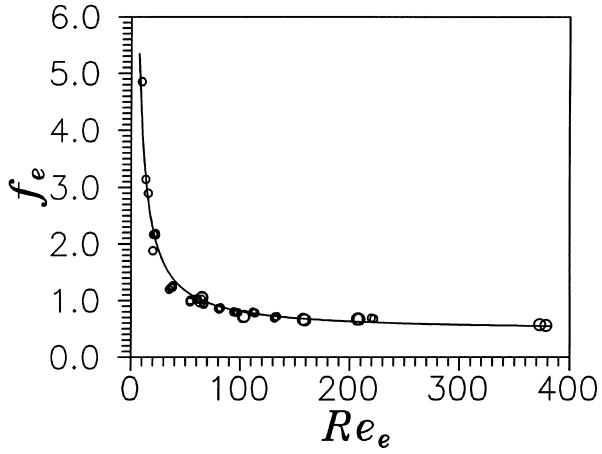

Fig. 6. Friction factor in the porous plate channel: ◯ – experimental results; –– calculated using Eq. (13).

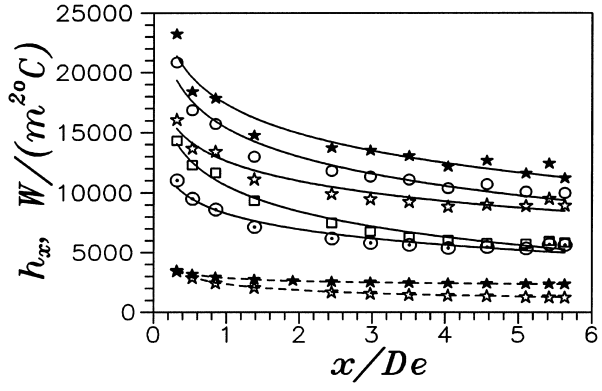

Fig. 7. Local heat transfer coefficients for glass packed beds ($d_p = 0.428$ mm, $\varepsilon_m = 0.366$). ⊙, □, ☆, ◯, ★ –– experimental data; - - - - - predicted values for empty plate channel G[kg/s], Re_D: ⊙ – 0.0345, 735; □ – 0.0555, 1196; ☆ – 0.0825, 1778; ◯ – 0.1108, 2376; ★ – 0.1982, 4284.

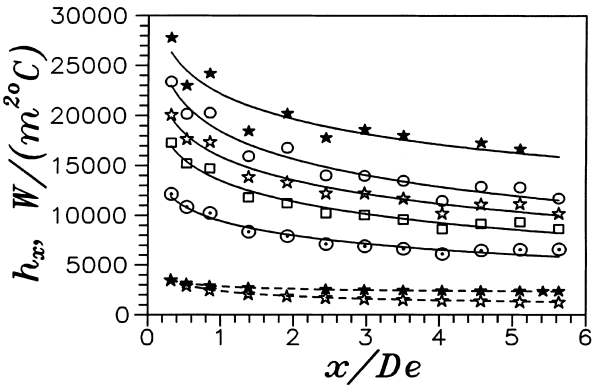

Fig. 8. Local heat transfer coefficients for stainless steel packed beds ($d_p = 0.428$ mm, $\varepsilon_m = 0.365$. ⊙, □, ☆, ◯, ★ –– experimental data; ----- predicted values for empty plate channel G[kg/s], Re_D: ⊙ – 0.0311, 691; □ – 0.0719, 1681; ☆ – 0.0838, 1889; ◯ – 0.1006, 2187; ★ – 0.1964, 4257.

especially for high flow velocities. However, the higher hear transfer coefficients are accompanied by sharply increased flow resistance in the porous plate channels as the particle diameter decreases, Fig. 5. Therefore, optimum particle diameters should be used to enhance the heat transfer with moderate pressure drop.

3.4. Effect of particle thermal conductivity on heat transfer

Figs. 10, 11 show the experimental data for the local and mean heat transfer coefficients in the plate channel filled with glass beads or with stainless steel or bronze particles. Increasing the particle thermal conductivity increased the local and the mean heat transfer coefficients. Quantitative analysis of the effect of particle thermal conductivity on the heat transfer coefficient needs further work, as pointed out by Jeigarnik et al. [9].

As is evident in Fig. 11, the difference between the mean heat transfer coefficients for different particle materials increased with increasing Reynolds number.

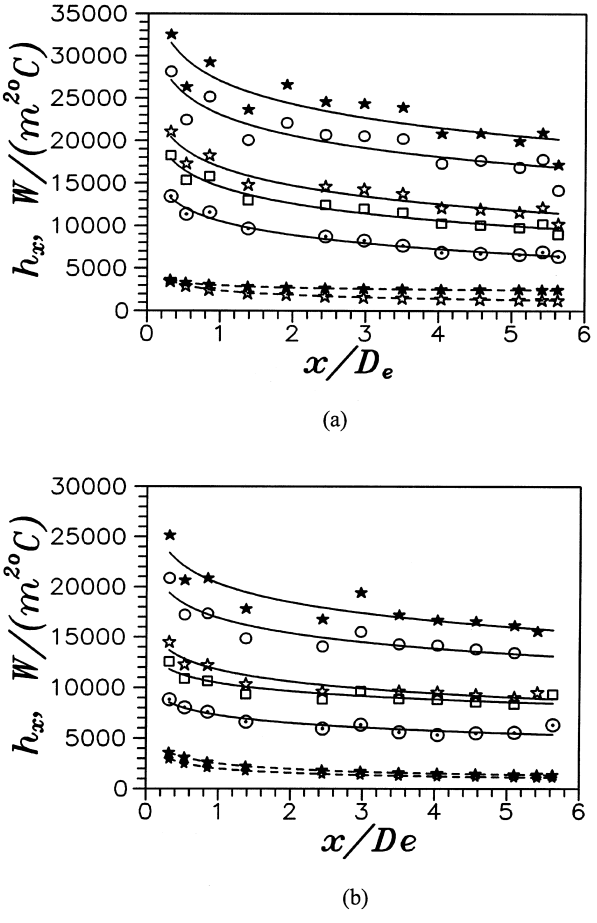

Fig. 9. Local heat transfer coefficients for bronze packed beds. ⊙, □, ☆, ◯, ★ –– experimental data; ----- predicted values for empty plate channel; (a) ($d_p = 0.428$ mm, $\varepsilon_m = 0.365$ G[kg/s], Re_D: ⊙ – 0.0310, 743; □ – 0.0721, 1650; ☆ – 0.0831, 1918; ◯ – 0.1266, 2966; ★ – 0.1964, 4507; (b) ($d_p = 0.278$ mm, $\varepsilon_m = 0.341$ G[kg/s], Re_D: ⊙ – 0.0157, 357; □ – 0.0312, 715; ☆ – 0.0539, 1195; ◯ – 0.0771, 1709; ★ – 0.0948, 2096.

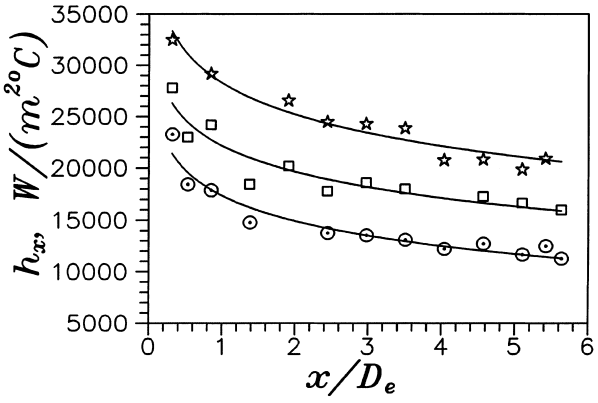

Fig. 10. Effect of particle thermal conductivity on local heat transfer coefficient ($d_p = 0.428$ mm), ☆ – bronze particles; $\varepsilon_m = 0.365$; $G = 0.1964$ kg/s; □ – stainless steel particles; $\varepsilon_m = 0.365$; $G = 0.1964$ kg/s; ⊙ – glass particles; $\varepsilon_m = 0.366$; $G = 0.1982$ kg/s.

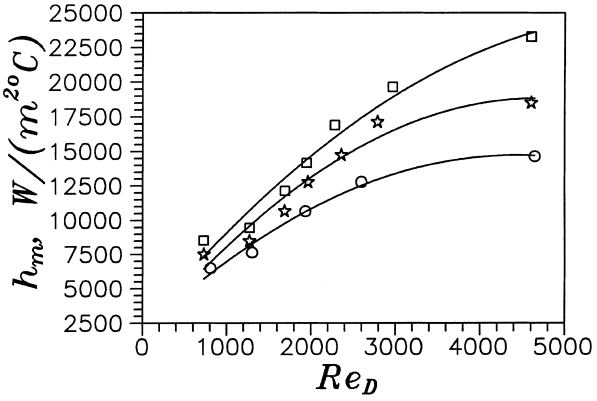

Fig. 11. Effect of particle thermal conductivity on mean heat transfer coefficient $d_p = 0.428$ mm, □ – bronze particles; $\varepsilon_m = 0.365$; ☆ – stainless steel particles; $\varepsilon_m = 0.365$; ◯ – glass particles; $\varepsilon_m = 0.366$.

Therefore, using metallic particles with high thermal conductivity enhances the heat transfer more effectively at high Reynolds numbers. This can be explained as follows: the convection heat transfer process in the porous plate channels is controlled by two factors, the convection heat transfer between the fluid and the channel surface, and the "fin effect" of the particles which intensifies with increasing particle thermal conductivity and Reynolds number. The "fin effect" of the particles is controlled by the combined effects of the convection heat transfer between the fluid and the particles and the thermal conduction between the particles. For low Reynolds numbers, the thermal conduction resistance across particles with low thermal conductivity is close to the convection heat transfer resistance between the fluid and the particles, so the influence of the particle thermal conductivity on the "fin effect" of the particles is not very large. Therefore, for low Reynolds numbers in porous plate channels, the difference between the heat transfer coefficient on the heated plate channel surface for different particle materials is not large, as shown in Figs. 7–9,11. However, for high Reynolds numbers, the convection heat transfer resistance between the fluid and the particles may be much less than the thermal conduction resistance across particles with low thermal conductivity (e.g., glass beads), so the low thermal conductivity of the particles weakens the "fin effect" of the particles. For packed beds with high thermal conductivity particles, the thermal conduction resistance between particles may be not greater than the convection heat transfer resistance between the fluid and the particles even for high Reynolds number; so, the "fin effect" of the particles is always important. Therefore, the heat transfer coefficient along the heated plate channel surface for metallic packed beds is much higher than that for glass packed beds when the Reynolds number in the porous plate channels is large, as shown in Figs. 7–9,11. Consequently, for heat transfer enhancement, high thermal conductivity metallic particles are more effective than glass particles, especially for high Reynolds number flow.

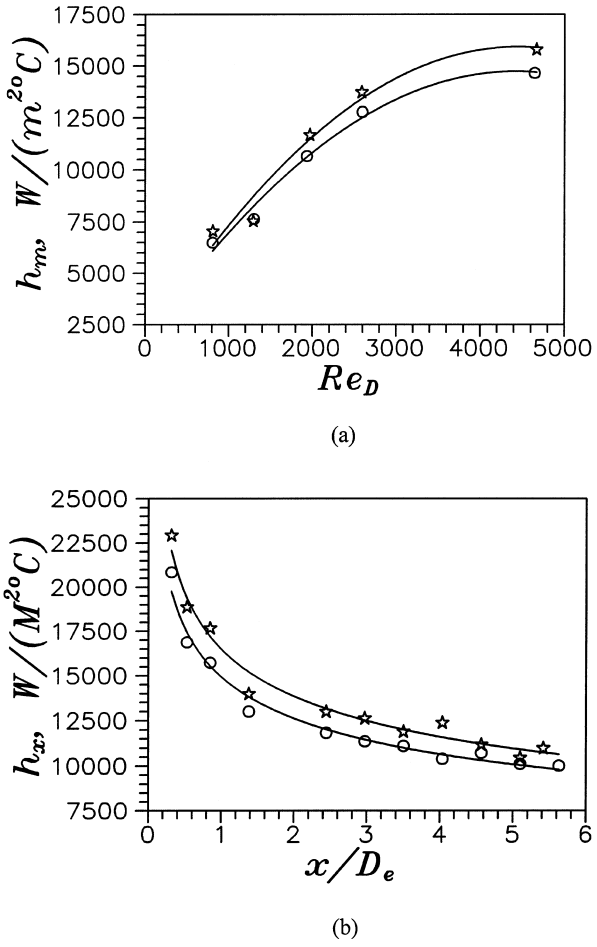

Fig. 12. Effect of particle diameter on (a) mean and (b) local heat transfer coefficient for glass packed beds. (a) ☆ – $d_p = 0.7$ mm, $\varepsilon_m = 0.378$; ○ – $d_p = 0.428$ mm, $\varepsilon_m = 0.366$; (b) ☆ – $d_p = 0.7$ mm, $\varepsilon_m = 0.378$, $G = 0.1104$ kg/s; ○ – $d_p = 0.428$ mm, $\varepsilon_m = 0.366$, $G = 0.1108$ kg/s.

3.5. Effect of particle diameter on heat transfer

Figs. 12–14 show the effect of particle diameter on the local and mean heat transfer coefficients for glass, stainless steel and bronze packed beds. For the conditions studied, the heat transfer coefficients for porous plate channels filled with glass particles increased with increasing particle diameter which corresponds to the results in [13–15,18]. However, for porous plate channels filled with stainless steel or bronze particles, the heat transfer coefficients increased with decreasing particle diameter which agrees with the experimental results in [9–11]. The opposite trends result from the competing factors of the mixing effect (or thermal dispersion) and the decreased contact surface area between particles as the particle diameter increases. For glass packed beds, the thermal conductivity is comparable to water so that the thermal dispersion is the dominant effect for the conditions studied. The thermal dispersion effect increases with increasing particle diameter, therefore, the heat transfer increases with increasing particle diameter for glass packed beds. However, for metallic packed beds, the particle thermal conductivity is much higher than water, thus, thermal conduction through the solid particles and convection heat transfer between the particles and the water (the "fin effect") play a very important role in the overall convection heat transfer on the plate channel surface. The contact surface area between the particles and the water increased with decreasing particle diameter, which intensified the convection heat transfer. Therefore, for the conditions studied, the heat transfer coefficients increased with decreasing particle diameter for metallic packed beds.

In fact, the effect of solid particle diameter on the convection heat transfer is much more complicated. A previous work [19] theoretically and numerically analyzed the effect of solid particle diameter on the convection heat transfer. The results showed that the

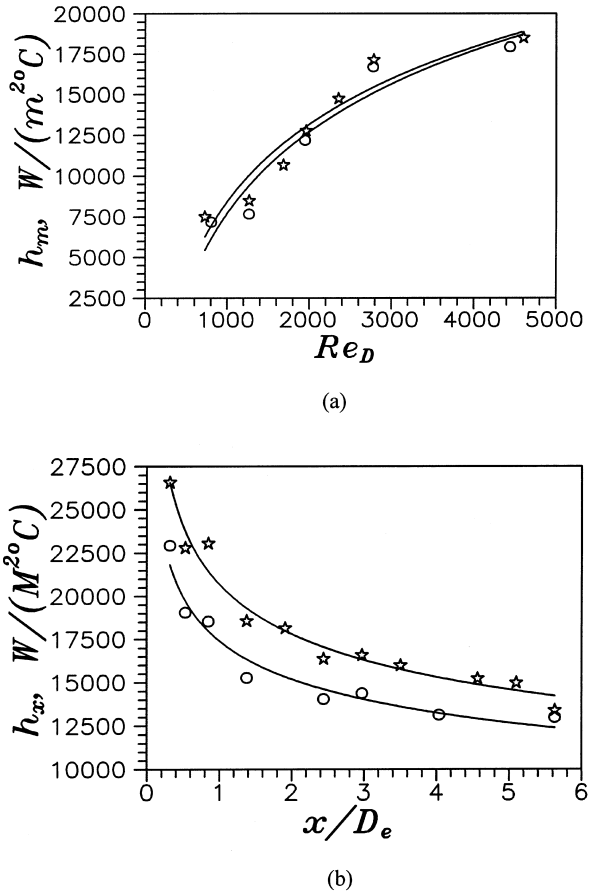

Fig. 13. Effect of particle diameter on (a) mean and (b) local heat transfer coefficient for steel packed beds. (a) ☆ – $d_p = 0.428$ mm, $\varepsilon_m = 0.365$; ◯ – $d_p = 0.7$ mm, $\varepsilon_m = 0.379$; (b) ☆ – $d_p = 0.428$ mm, $\varepsilon_m = 0.365$, $G = 0.1189$ kg/s; ◯ – $d_p = 0.7$ mm, $\varepsilon_m = 0.379$, $G = 0.1186$ kg/s.

convection heat transfer coefficient on the heated channel surface can decrease or increase as the particle diameter increases depending on the values of $\varepsilon, k_s, k_f, k_d, \rho u$, etc. A criterion for judging the variation of the convection heat transfer coefficients as d_p increases as presented in [19] based on an earlier thermal dispersion conductivity model. In [24] we presented a new modified thermal dispersion conductivity model. A modified approximate criterion was then developed using the new modified thermal dispersion conductivity model.

When

$$\rho_0 u_0 d_p > 0.787 \frac{k_{eff}^{5.82}}{c_{pf}} \frac{\varepsilon_m}{1-\varepsilon_m}. \tag{14}$$

The convection heat transfer coefficient on the heated channel surface, h_w, increases as d_p increases. Otherwise, h_w increases as d_p decreases.

This criterion is verified by the present experimental results, Fig. 15. For the glass particles, which satisfy Eq. (14), h_w was shown to increase as d_p increased, Fig. 12. For bronze particles which do not satisfy Eq. (14), h_w as shown to increase as d_p decreased, Fig. 14. For stainless

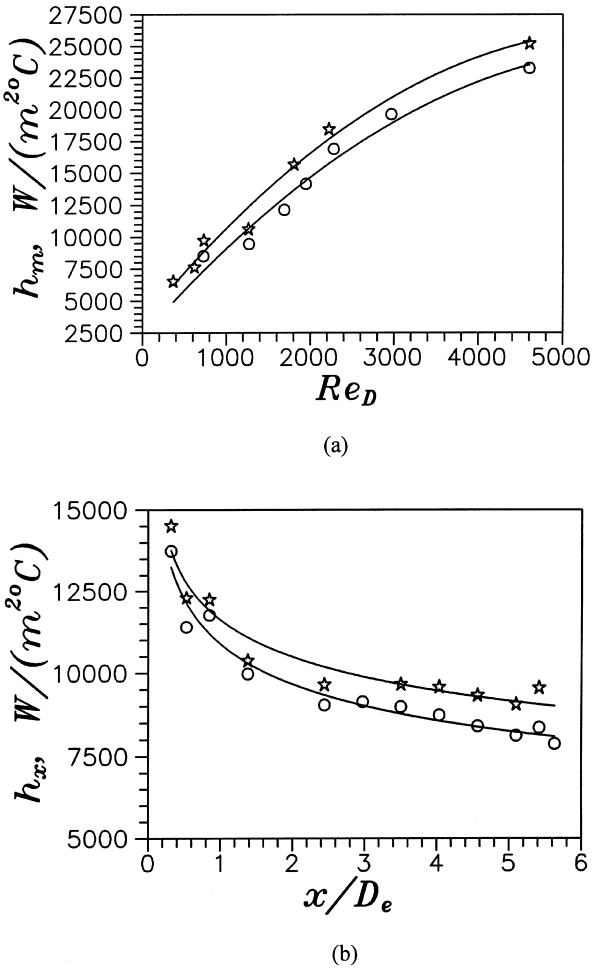

Fig. 14. Effect of particle diameter on (a) mean and (b) local heat transfer coefficient for bronze packed beds. (a) ☆ – $d_p = 0.278$ mm, $\varepsilon_m = 0.341$; ◯ – $d_p = 0.428$ mm, $\varepsilon_m = 0.365$; (b) ☆ – $d_p = 0.278$ mm, $\varepsilon_m = 0.341$, $G = 0.0539$ kg/s; ◯ – $d_p = 0.428$ mm, $\varepsilon_m = 0.365$, $G = 0.0542$ kg/s.

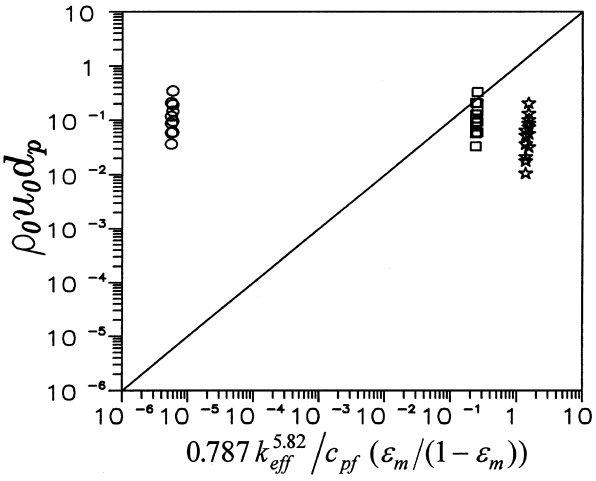

Fig. 15. Experimental data for judging the effect of particle diameter. ☆ – bronze particles; □ – stainless steel particles; ◯ – glass particles.

steel particles most of the data points do not satisfy Eq. (14) so h_w increased as d_p decreased. But for larger mass flow rates in the stainless steel packed beds, Eq. (14) is satisfied and h_w increased as d_p increased, Fig. 13. Considering the experimental uncertainty of the present work, the approximate criterion given by Eq. (14) and the analysis correspond well to the experimental results depicted in Figs. 12–14.

4. Practical significance

Packed beds greatly increase the heat transfer coefficient showing that porous structures are an effective heat transfer augmentation technique. However, the flow resistance in porous medusa is very large. Therefore, porous structures can be used in some special cases for enhancing heat transfer, such as in cooling systems for powerful laser mirrors, aerospace craft, thermal nuclear fusion, phased-array radar systems, micro heat exchangers, etc. where high heat transfer rates are of critical importance. Since the heat transfer is an complex function of the particle thermal conductivity and the particle diameter in the porous channels, the results in the present work can be used to effectively optimize the heat transfer augmentation design.

The experimental data can also be used for checking physical–mathematical models or numerical results for convection heat transfer in porous media.

5. Conclusion

Forced convection heat transfer in a plate channel filled with glass, stainless steel or bronze spherical particles was investigated experimentally. The main results can be summarized as:

1. The pressure drop was greatly increased by the porous media and increased as the particle diameter decreased. The experimental results for friction factor, f_e, obtained in this paper agree well with the existing correlation equation given by Eq. (13).
2. For porous plate channels filled with glass particles, the heat transfer coefficient increased with increasing particle diameter; but for porous plate channels filled with bronze particles, the heat transfer coefficient increased with decreasing particle diameter.
3. Increasing the particle thermal conductivity caused the heat transfer coefficient to increase. The difference between the heat transfer coefficients for different particle materials increased with increasing Reynolds number.
4. The packed bed greatly increased the heat transfer coefficient. Packed beds with smaller bronze particles gave the highest heat transfer coefficients, but the flow resistance in the porous plate channels increased sharply as the particle diameter decreased. Therefore, an optimum particle diameters should be selected to enhance the heat transfer with a moderate pressure drop.

6. Recommendations and future research needs

The present work used only one heated test selection (58 mm × 80 mm × 5 mm). Further work is needed to assess the effect of channel size (especially the ratio of the particle diameter to the height of the channel) on the heat transfer. In addition, experiments using other particle materials and more particle diameters are needed to further clarify these effects. Convection heat transfer in sintered porous channels should also be investigated and compared with the heat transfer results in packed beds. Different structures of the porous channel including the direction of the inlet and the number of inlets may also affect the heat transfer.

Nomenclature

A	area of the heated test section, m^2
c_{pf}	fluid specific heat, J(kg K)
d_p	particle diameter, m
D_e	equivalent diameter of the porous plate channel, m
G	mass flow rate, kg/s
h	channel height, m
h_x	local heat transfer coefficient, W/(m^2 K)
h_m	mean heat transfer coefficient, W/(m^2 K)
k	thermal conductivity of the test section material, W/(m K)
k_d	dispersive component of thermal conductivity of fluid and porous media, W/(m K)
k_{eff}	stagnant effective thermal conductivity of fluid and porous media, W/(m K), equation given in Ref. [18,19]
k_f	fluid thermal conductivity evaluated at the local film temperature T_{fb}, W/(m K)
k_m	fluid thermal conductivity evaluated at the mean temperature T_{fm}, W/(m K)
k_s	solid particle thermal conductivity, W/(m K)
L	channel length, m
M	mass flux, ($=\rho u$), kg/(m^2 s)
p	pressure, Pa
Δp	pressure drop, Pa
Pr	Prandtl number (dimensionless)
Q	power input, W
q_w	heat flux, ($=Q$/A), W/m^2
Re_e	equivalent Reynolds number, $(2Md_p/(3\mu_f(1-\varepsilon)))$ (dimensionless)
T_{fb}	local bulk temperature of the fluid, °C
T_{fm}	mean temperature of the fluid in the plate channel, °C
T_{wm}	mean temperature of the heat transfer surface, °C
T_{wx}	local temperature of the heat transfer surface, °C
T_x	measured temperature in the experiment, °C
V_P	volume of solid particles in the porous channel, m^3
V_t	total porous channel volume, m^3
u	fluid velocity in the x direction, m/s
W	channel width, m
x,y	coordinates in the flow region, m

Greek symbols

ν_m	kinematic viscosity of the fluid evaluated at the mean fluid temperature, m^2/s
ρ	fluid density, kg/m^3
ε_m	mean porocity, [dimensionless]
δ	distance between the temperature measurement point to the convection heat transfer surface, ($=0.5$ mm), m
Δx	distance between adjacent thermocouples, m

Subscripts

O	heated section inlet
b	bulk mean temperature
f	fluid
in	test section inlet
out	test section outlet
w	wall

Acknowledgements

The project was financially supported by the National Natural Science Foundation of China (No. 59506004), the Fund for Excellent Young University Teachers of the State Education Committee of China and the Natural Science Fundamental Research Foundations of Tsinghua University, Beijing, China.

References

[1] D.B. Tuckerman, R.F. Pease, High performance heat sinking for VLSI, Electron Device Lett. 2 (1981) 126–129.

[2] D.B. Tuckerman, R.F. Pease, Ultra high thermal conductance microstructures for cooling integrated circuits, IEEE, ch. 781-4 (1982) 145–149.

[3] M. Mahalingam, Thermal management in semiconductor device packaging, Proc. IEEE 73 (1985) 1396–1404.

[4] V.V. Haritonov, U.N. Kiceleva, V.V. Atamanov, U.A. Jeigarnik, F.P. Ivanov, Generalization of the Results on Heat Transfer Intensification in Channels with Porous Insertion (in Russian), Teplofizika Vys. Temp. 32 (3) (1994) 433–440.

[5] V.I. Subbojin, V.V. Haritonov, Thermophysics of Cooled Laser Mirrors (in Russian), Teplofizika Vys. Temp. 29 (2) (1991) 365–375.

[6] J.L. Lage, A.K. Weinert, D.C. Price, R.M. Weber, Numerical study of a low permeability microporous heat sink for cooling phased-array radar systems, Int. J. Heat Mass Transfer 39 (17) (1996) 3633–3647.

[7] G.M. Chrysler, R.E. Simons, An experimental investigation of the forced convection heat transfer characteristics of fluorocarbon liquid flowing through a packed-bed for immersion cooling of microelectronic heat sources, in: AIAA/ASME Thermophysics and Heat Transfer Conference, Cryogenic and Immersion Cooling of Optics and Electronics Equipment, ASME HTD, vol. 131, 1990, pp. 21–27.

[8] S.M. Kuo, C.L. Tien, Heat transfer augmentation in a foam-material filled duct with discrete heat sources, in: Intersociety Conference on Thermal Phenomena in the Fabrication and Operation of Electronic Components, IEEE, New York, pp. 87–91, 1988.

[9] U.A. Jeigarnik, F.P. Ivanov, N.P. Ikranikov, Experimental Data on Heat Transfer and Hydraulic Resistance in Unregulated Porous Structures (in Russian) Teploenergetika, vol. 21, 1991, pp. 33–38.

[10] G.H. Hwang, C.H. Chao, Heat transfer measurement and analysis for sintered porous channels, J. Heat Transfer 116 (1994) 456–464.

[11] K. Nasr, S. Ramadhyani, R. Viskanta, An experimental investigation on forced convection heat transfer from a cylinder embedded in a packed bed, J. Heat Transfer 116 (1994) 73–80.

[12] C.Y. Choi, F.A. Kulacki, Non-darcian effects on mixed convection in a vertical porous annulus, in: Proceedings of the Nineth IHTC-Heat transfer, Hemisphere, New York, vol. 5, 1990, pp. 271–276.

[13] N.J. Kwendakwema, R.F. Boehm, Parametric study of mixed convection in a porous medium between vertical concentric cylinders, J. Heat Transfer 113 (1991) 128–134.

[14] B.X. Wang, J.H. Du, Forced convective heat transfer in a vertical annuli filled with porous media, Int J. Heat Mass Transfer 36 (1993) 4207–4214.

[15] E. David, G. Lauriat, P. Cheng, A numerical solution of variable porosity effects on natural convection in a packed-sphere cavity, J. Heat Transfer 113 (1991) 391–399.

[16] C.T. Hsu, P. Cheng, Thermal dispersion in a porous medium, Int. J. Heat Mass Transfer 33 (8) (1990) 1587–1597.

[17] R. Clarksean, R. Golightly, R.F. Boehm, An experimental and numerical investigation on mixed convection in a porous medium between vertical concentric cylinders, in: Proceedings of the Nineth IHTC-Heat Transfer, Hemisphere, New York, vol. 2, 1990, pp. 477–482.

[18] P.X. Jiang, B.X. Wang, D.A. Luo, Z.P. Ren, Fluid flow and convective heat transfer in a vertical porous annulus, Numerical Heat Transfer Part A 30 (3) (1996) 305–320.

[19] P.X. Jiang, Z.P. Ren, B.X. Wang, Z. Wang, Forced convective heat transfer in a plate channel filled with solid particles, J. Thermal Sci. 5 (1) (1996) 43–53.

[20] E. Achenbach, Heat and flow characteristics of packed beds, Experimental Thermal and Fluid Science 10 (1996) 17–27.

[21] B.S. Petukhov, L.G. Genin, S.A. Kovalev, Heat Transfer in Nuclear Power Equipment (in Russian) Energoatomizdat Press, Moscow, 1996.

[22] V.A. Grigoriev, V.M. Zorin (Eds.), Theoretical Basis of Thermal Technology (in Russian), Second Ed., Moscow Energoatomizdat Press, Moscow, 560, 1988.

[23] M.E. Aerov, O.M. Tojec, Hydraulic and Thermal Basis on the performance of Apparatus with Stationary and Boiling Granular Layer (in Russian) Himia Press, Leningrad, 1968.

[24] P.X. Jiang, Z.P. Ren, B.X. Wang, Numerical Simulation of Forced Convection Heat Transfer in Porous Plate Channels Using Thermal Equilibrium and Non-Thermal Equilibrium Models, submitted to Numerical Heat Transfer, Part A 35 (1) (1999) 99–113.